IOP Conference Series:
Materials Science and
Engineering

PAPER • OPEN ACCESS

Numerical investigation of a pressure wave supercharger

To cite this article: I Costiuc and L Costiuc 2022 *IOP Conf. Ser.: Mater. Sci. Eng.* **1220** 012022

Numerical investigation of a pressure wave supercharger

I Costiuc[1], L Costiuc[2]

[1]Automotive and Transport Engineering Department, Faculty of Mechanical Engineering, Transilvania University of Brașov, BV 500036, Romania
[2]Mechanical Engineering Department, Faculty of Mechanical Engineering, Transilvania University of Brașov, BV 500036, Romania

costiuciuliana@unitbv.ro

Abstract. The paper aims at a numerical investigation of the evolution of velocity, pressure and temperature field along the wave rotor channels for a pressure wave supercharger. Since in literature most of the studies are made considering the working fluid as incompressible and inviscid in a 2D field, the present study is using the compressible and viscous terms in unsteady Navier-Stokes equations for fluid in 3D field. The geometry was drawn in CAD software using measurements made on a real model of the CX-93 pressure wave supercharger. The simulation was conducted using a CFD code for unsteady 3D k-ε, k-ω model approach to reproduce data such as pressures, temperature and mass flows which are usually measured in real engine pressure wave supercharging. The computational domain for uRANS was modeled as a moving rotational domain with adaptive meshing. Results such as velocity, pressure and temperature field in the rotor channels were obtained for exhaust gas inlet pressure of 0.28 MPa and 1465 K temperature at different rotational speeds. The air inlet state considered was: 0,098 MPa and 293 K. Supercharging by means of a pressure wave supercharger, in order to improve the performance of an internal combustion engine, appears to be a promising solution since the exhaust gas generates a benefice boost of intake air with significant advantages when compared to the conventional turbocharging. The numerical modelling of the complex phenomena occurring within the narrow channels might be a useful tool for improving the pressure exchange between the working fluids, either by modifying the input parameters or by optimizing the geometry of the rotor, ports or pockets.

1. Introduction

The European Union established as one of its key targets for 2020 a 20% reduction in greenhouse gas emissions compared with 1990, and a 40% reduction for 2030 [1]. Consequently, the EU has taken legislative action to restrict higher levels of pollution, especially arising from burning fossil fuels. The primary consumers of fossil fuels are the propulsion systems, being stated [2] that the road transportation sector is one of the main sources of greenhouse gas emissions, e.g. CO_2, and air pollutants. Therefore, the internal combustion engines (ICE) have become the point of interest in terms of reducing emissions, as well as efficient use of energy.

Among the measures to reduce vehicle emissions EU, the most common are: the introduction of alternative propulsion technologies - by developing the hybrid or electric cars; eco-innovation; improving the efficiency of conventional engines - by implementing advanced and specific technologies, such as technologies for the exhaust system: oxidation catalysts, cellular filters, absorbers, catalysts substances injected into the gas stream, etc. Well-conceived thermal management of the ICE can contribute in achieving the targets outlined above, by:

- energy conservation and waste heat recovery,
- improving the overall efficiency and performance,
- lowering fuel consumption and, thus,
- reducing gas emissions.

Supercharging aims to increase the torque and engine power by raising bmep while reducing the maximum engine speed. Thus, the mechanical losses of the engine, the noise and fuel consumption decrease, with the benefit of prolonging engine life [3]. Superchargers are efficient in low and medium engine speeds, but their improvement on thermal efficiency is very limited because the effective work is reduced with the amount consumed to drive the compressor. On the other hand, turbochargers have higher thermal efficiency because the compressor is driven by the energy coming from the exhaust gases, but they work properly on the engine high-speeds range and they induce increased exhaust gas pressures.

2. Pressure Wave Supercharging

2.1. Fundamentals of PWS. General Operating Principles. Design and Construction

A PWS operation is based on the pressure waves ability to transfer energy from the combustion gases to the intake air. The PWS geometry consists of a rotor (called wave rotor or cell wheel) with channels shaped parallel to the rotation axis, which are radially positioned on one or more rows (Fig.1a). The PWS, by means of shockwaves, transfer the energy inside the channels directly from the exhaust gas towards the fresh intake air, the fluids being in short direct contact.

The fluids are the high pressure hot gases (HPG) and the low pressure cold air (LPA), and their interaction induces boost, as the exhaust gases compress the intake fresh air. Within the channels the process is extremely fast, thus, the phenomenon of mixing between the two fluids is insignificant.

The cell wheel rotates inside a casing, in between two fixed end plates (figure 1a.): one connected to the intake manifold, called the “cold stator” (figure 1b.) and one connected to the exhaust gas passages, called the “warm stator” (figure 1c.). The rotor is driven by a pulley-belt drive mechanism that rotates the cell wheel with a multiple of the engine speed [3].

(a) (b) (c)

Figure 1. (a) rotor, also named cell wheel, (b) warm stator, (c) cold stator.

The acoustic and thermodynamic processes between the inlet fluids result in the outlet fluids leaving the PW supercharger: the low pressure gases (LPG) leaving the rotor towards the exhaust system and the compressed high pressure air (HPA) heading towards the cylinders (figure 2).

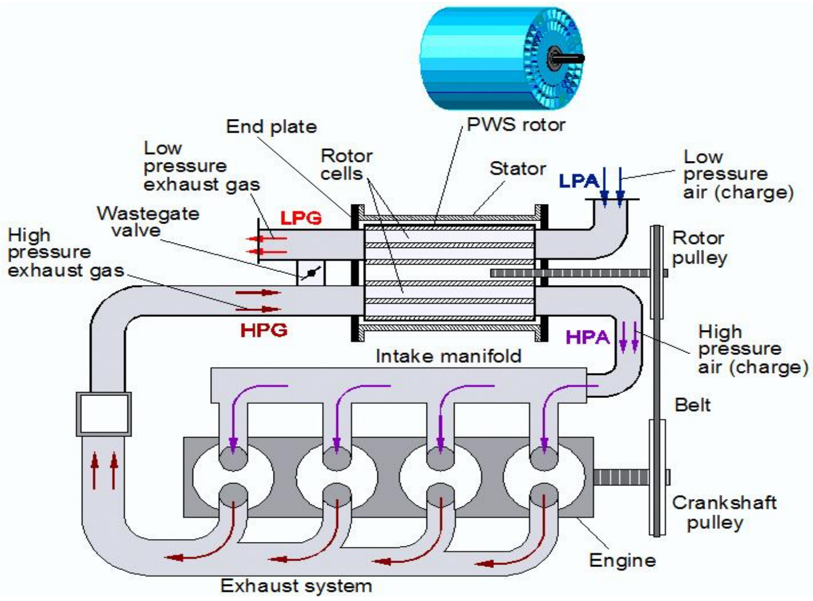

Figure 2. Four port PWS working fluids and assembly elements.

The configuration with four end plates that contain the inlet and outlet ports consists of: two ports for the exhaust gases (HPG and LPG), and two ports for the air (LPA and HPA). PWS can be designed as shown in figure 3 in two configurations: passing-through flow (TF) - when the working fluids flow in the same direction, and reverse flow (RF) - when each fluid enters and exits on the same side.

These two configurations ensure similar performance values but they are substantially different. In the 4 ports TF rotor, both fluids travel the rotor longitudinally, maintaining an average temperature relatively constant over the entire length of the rotor, allowing a self-cooling effect to the rotor. On the RF configuration, the air casing remains cold while the gases casing gets hot, being suitable for other types of applications [5]. In this paper, a RF configuration is used for the numerical modelling of the PWS operation.

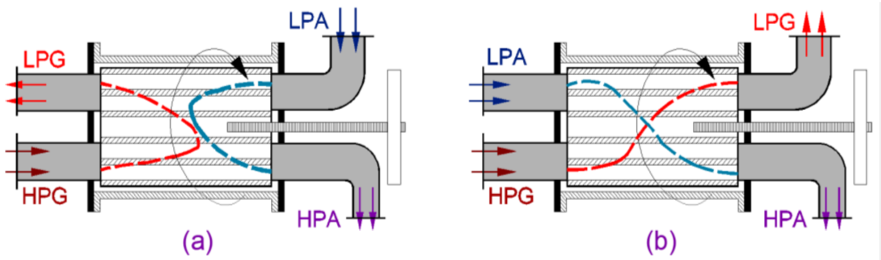

Figure 3. Four port PWS configurations [4]:
(a) The passing-through flow configuration, (b) The reverse flow configuration.

In short terms, the PWS rotor, as it rotates, allow the channel openings to be exposed alternatively to the inlet or outlet openings, therefore the fluids flow through the ports. The compression and expansion waves are initiated inside the rotor channels; the pressure waves evolving inside the channels compressing the intake charge.

In practice, the PWS design is rather difficult, concerning the number of channels, the number of rows or, for instance, breaking the symmetry of the rotor cells for reducing the noise [4-9]. Also, the leakage is of great importance as it seriously affects the performance – it has to be minimized, yet preventing the occurrence of contact, regardless of the thermal regime. A 0.5mm gap was taken into account in the present model design.

3. Pressure Wave Supercharger Modelling and Calculations

3.1. Introduction
In order to model the pressure wave compressor processes, we need to build the basic equations based on fundamental physical principles for viscous flow, choose a suitable model of the fluid and obtain mathematical equations, which properly describe the physics of the flow. In this part, the equations are be presented for unsteady, compressible and viscous three-dimensional flow in a general form. The viscous approach was chosen because the effects of viscosity, thermal conduction, and mass diffusion are important. Also, particularized models for pressure wave compressor used during the years are presented after the general model. The steps for mathematical modeling usually are:

I. *State three fundamental physical principles of nature, namely:*
a. Mass is conserved (i.e., mass can be neither created nor destroyed).
b. Newton's second law: force = mass × acceleration.
c. Energy is conserved; it can only change from one form to another.
II. *Determine a suitable model of the fluid:* the finite control volume, the infinitesimal fluid element and molecular model.
III. *Apply the fundamental physical principles to the chosen model of the fluid* in order to obtain mathematical equations which properly describe the flow.

3.2. The equations of compressible viscous flow
A complete set of equations presented in the differential form below are the compressible Navier-Stokes equations for an isotropic Newtonian fluid with variable properties [11, 12]. The first three equations are conservation of mass, momentum and energy, and the rest of the equations are constitutive equations to complete the model.

$$\frac{D\rho}{Dt} + \rho\nabla \cdot V = 0 \quad \text{(1 eq.)}$$
$$\rho\frac{DV}{Dt} = -\nabla p + \rho f + \nabla \cdot \tau \quad \text{(3 eqs.)}$$
$$\rho\frac{D}{Dt}\left(e + \frac{1}{2}V \cdot V\right) = \rho\dot{q}_{gen} - \nabla \cdot \dot{q}_{visc} - \nabla \cdot (pV) + \rho(f \cdot V) + \nabla \cdot (\tau \cdot V) \quad \text{(1 eq.)}$$
$$\tau = \mu\left(\nabla V + \nabla V^T\right) + \lambda(\nabla \cdot V)I \quad \text{(6 eqs.)}$$
$$\dot{q}_{visc} = \dot{q}_{cond} = -k\nabla T \quad \text{(3 eqs.)}$$
$$\dot{q}_{gen} = 0 \quad \text{(0 eq., if neglected)}$$
$$\mu = \mu(\rho, T) \quad \text{(1 eq.)}$$
$$\lambda = \lambda(\rho, T) \quad \text{(1 eq.)}$$
$$k = k(\rho, T) \quad \text{(1 eq.)}$$
$$p = p(\rho, T) \quad \text{(1 eq.)}$$
$$e = e(\rho, T) \quad \text{(1 eq.)}$$

The unknown variables of the above differential system are:

- ρ – density, scalar, 1 variable [kg m^{-3}]
- $\boldsymbol{V}$ – velocity, vector, 3 variables [m s^{-1}]
- p – pressure, scalar, 1 variable [N m^{-2}]
- e – internal energy, scalar, 1 variable [J kg^{-1}]
- T – temperature, scalar, 1 variable [K]
- τ – viscous stress, symmetric tensor, 6 variables [N m^{-2}]
- $\boldsymbol{q}_{cond}$ – heat flux vector, vector, 3 variables [W m^{-2}]
- μ – first coefficient of viscosity, scalar, 1 variable [kg $m^{-1}s^{-1}$]
- λ – second coefficient of viscosity, scalar, 1 variable [kg $m^{-1}s^{-1}$]
- k – thermal conductivity, scalar, 1 variable [W $m^{-1}K^{-1}$]

The volumetric body force considered in most models is given only by a gravitational field and there f = g and is the constant gravitational acceleration. The result is a differential system with 19 equations and 19 variables, which can be solved. But, this system must be and become consistent with considering the second law of thermodynamics that states:

$$\rho \frac{Ds}{Dt} \geq -\nabla \cdot \left(\frac{\dot{q}_{ht}}{T}\right)$$

and the result is:

$$-\frac{\dot{q}_{ht}}{T^2}\nabla T + \frac{1}{T}(\tau : \nabla V) \geq 0$$

The constitutive equations for thermal conductivity $k(\rho, T)$, or heat flux $\dot{q}_{ht}$, first viscosity coefficient $\mu(\rho, T)$, the second viscosity coefficient $\lambda(\rho, T)$ and then the viscous stress τ must be constructed and verified as that to respect the second law of thermodynamics.

4. Numerical model

In the present work, the PWS geometry was created in a 3-D model using ACAD software and was imported into Comsol software [13, 14] (see figure 4). The model uses baseline dimensions for Comprex CX-93 four port reverse flow pressure wave supercharger. The mesh resulted after some geometry repair operations are presented in figure 5 consisting of 2386820 tetrahedral elements only on the air domain after meshing.

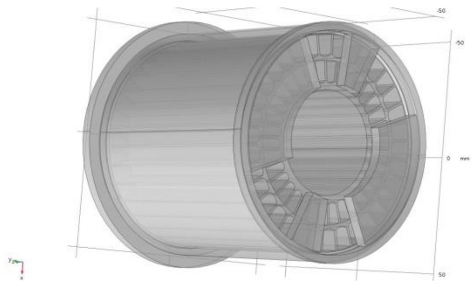

Figure 4. PWS imported geometry.

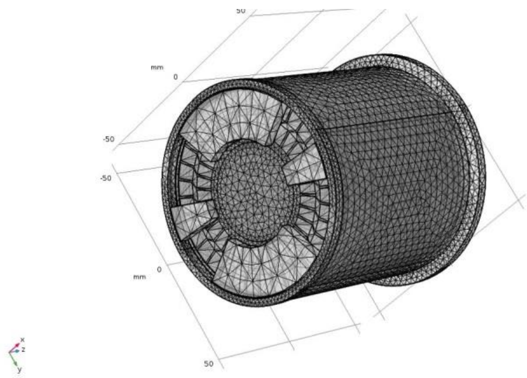

Figure 5. PWS resulted mesh.

The rotor material was considered steel and the fluid used is the air, considered a compressible gas. The specific heat, thermal conductivity and viscosity were considered as temperature dependent.

The model uses the Reynolds-averaged Navier-Stokes (RANS) equations in the air domain. The properties for the fluid are the air at atmospheric pressure and for the solid those of steel. The air properties are considered as temperature dependent. The equations for air domain, which includes equations for turbulent kinetic energy k and for dissipation ε, are used for the rotating domain model. To simulate the PWS time dependent behaviour, a rotating domain model was used. The first step was the frozen rotor study to provide an initial guess for the velocity field and pressure in the 3D domain. In the second step, the flow was treated as turbulent and time dependent using the coupling of the conservation and momentum equations with the energy equation.

The boundary conditions at inlet and outlet ports were set up as: a velocity and pressure input on the gas ports, and a pressure input on fresh air ports. To the entire rotating domain, rotor domain containing fluid, an axial motion was set up with the rotational speed *n*. The boundary conditions are presented in table 1.

Table 1. Entry data for the model

Property	Value	um
Air inlet pressure	$0.98 \cdot 10^5$	N m^{-2}
Air inlet temperature	293 K	K
Exhaust gas inlet pressure	$1.80 \cdot 10^5$	N m^{-2}
Exhaust gas inlet temperature	1465	K
Air specific heat ratio	1.4	-
Air specific gas constant	287	J kg^{-1}K^{-1}
Channel length	93	mm
Rotor diameter	93	mm
Revolutions per time	12600	rpm

5. Results and conclusion

The 3D model results are presented below. Figure 6 presents the pressure distribution in PWS channels in a contour plot, as figure 7 shows the velocity field.

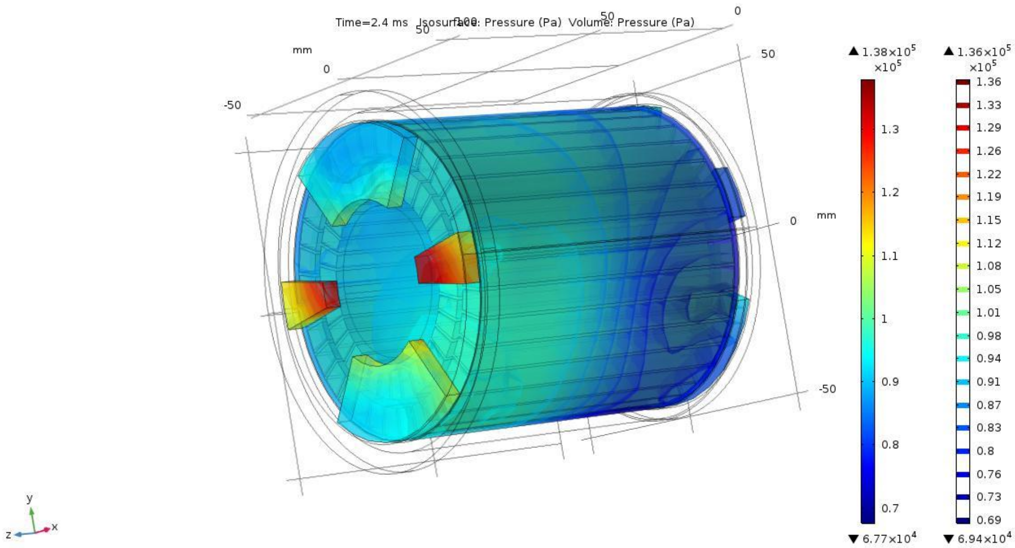

Figure 6. Pressure field @2.4ms time for 12600 rot/min.

The results obtained for the pressure on PWS air ports on the left side of figure 6 show that the compressed air at the moment of 2.4 msec. of time reaches the value of 1.36 bar on exit air ports. In figure 6 also are shown the resulting pressure field inside channels from exhaust gas inlets, the right side of the figure, to air side on the left. For the velocity field the results obtained are presented in figure 7. The PWS air ports are on the right side of figure 7 that shows that the exhaust gas enters with a maximum value of 75 m/s through inlet ports and travels to air side. Because of the rotating domain of the CX rotor, the velocity field is deflected from exhaust gas inlets to air ports. In figure 7 was shown the resulting velocity field inside channels from exhaust gas inlets, from the left side of the figure, to air side on the right side.

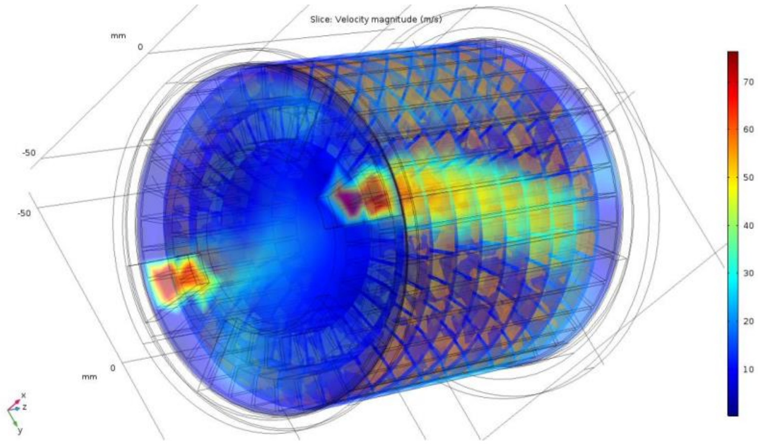

Figure 7. Velocity field @2.4ms time for 12600 rot/min.

As a conclusion, using a pressure wave supercharger to improve the performance of an internal combustion engine appears to be a promising solution since the exhaust gas generates an increase of air pressure on the aspired air, which has a beneficial effect on the internal combustion engine cycle. All theoretical and numerical results presented here encourage the idea that at microscale compression by pressure waves may be more efficient than by conventional mechanical compressors or turbochargers. The presented model can be used on other types of PWSs to enhance or optimize the engine performance or energy and ecological management.

References

[1] *** http://ec.europa.eu/clima/citizens/eu/index_ro.htm - European Comision - Climate Action
[2 *** http://www.eea.europa.eu/ EEA, 2015b, Monitoring CO_2 emissions from new passenger cars and vans in 2014. EEA Technical report No 16/2015, European Environment Agency.
[3] Heisler, H. - Advances Engine Technology, SAE International, 1995, ISBN 1560917342
[4] Fu JQ, Liu JP, Xu ZX, Ren CQ, Deng BL 2013 A combined thermodynamic cycle based on methanol dissociation for internal combustion engine exhaust heat recovery. Energy **55**, 778–86
[5] Fu J, Liu J, Wang Y, Deng B, Yang Y, Feng R, Yang J 2014 A comparative study on various turbocharging approaches based on IC engine exhaust gas energy recovery, App.Energ. **113**
[6] Spring P 2006 Modeling and Control of Pressure-Wave Supercharged Engine Systems, Diss. ETH No. 16490, Swiss Federal Institute of Technology, ETH Zurich
[7] Liu JP, Fu JQ, Ren CQ, Wang LJ, Xu ZX, Deng BL 2013 Comparison and analysis of engine exhaust gas energy recovery potential through various bottom cycles. Appl.Therm.Eng **50**
[8] Iancu F, Piechna J, Müller N 2008 Basic design scheme for wave rotors, Shock Waves **18**, Springer Verlag
[9] Frackowiak M, Iancu F, Potrzebowski A, Ackbari P, Müller N, Piechna J 2004 Numerical Simulation of Unsteady Flow Processes in Wave Rotors, Proc. of IMECE04 2004 ASME International Mechanical Engineering Congress, Anaheim, California USA
[10] Heywood J 1988 Internal Combustion Engine Fundamentals, McGraw-Hill International Editions
[11] Powers JM 2015 Lecture notes on gas dynamics. University of Notre Dame, USA
[12] Çengel YA, Boles MA 2006 Thermodynamics: An Engineering Approach, 5th edition, McGraw-Hill, 2006
[13] Costiuc I, Chiru A 2017 Thermodynamic Process Modeling in Pressure Wave Superchargers, RoJAE **23**, 83-88
[14] Comsol v.3.5a – Academic Licence